Materials Chemistry and Physics 209 (2018) 60–64

Contents lists available at ScienceDirect

Materials Chemistry and Physics

journal homepage: www.elsevier.com/locate/matchemphys

Field emission characteristics of basal plane and cross-sectional edges of graphite made from graphite oxide

Xiangyang Wang [a], Zezhang Yan [b], Zhuchen Tao [a], Ziqi Tan [a], Jianglin Ye [a], Fei Pan [a], Huailiang Xu [c], Yu Zhang [b], Shaozhi Deng [b], Yanwu Zhu [a, *]

[a] Key Laboratory of Materials for Energy Conversion, Chinese Academy of Sciences, Department of Materials Science and Engineering, i-ChEM, University of Science and Technology of China, 96 Jin Zhai Rd., Hefei, Anhui 230026, People's Republic of China
[b] State Key Laboratory of Optoelectronic Materials and Technologies, Guangdong Province Key Lab of Display Material and Technology, School of Electronics and Information Technology, Sun Yat-Sen University, Guangzhou 510275, People's Republic of China
[c] The Sixth Element (Changzhou) Materials Technology Co., Ltd., 9 West Tai Lake Avenue, Changzhou, Jiangsu 213000, People's Republic of China

HIGHLIGHTS

- Graphite is made from graphite oxide with well-defined basal plane and edges.
- The edges have demonstrated inferior field emission performance.
- The sparse wrinkles on the basal plane play important roles as emission sites.
- The oxygen-containing groups lead to deterioration in field emission performance.

ARTICLE INFO

Article history:
Available online 16 January 2018

Keywords:
Field emission
Basal plane
Edge
Graphite

ABSTRACT

Graphite made from graphite oxide with well-defined basal plane (perpendicular to the c-axis or stacking orientation) and cross-sectional edges (along to the stacking orientation) are utilized to investigate the field emission characteristics. The significant differences of basal plane and edges from the same graphite sample are characterized. It is found that the basal plane with wrinkles has lower turn-on field (5.01 V/μm, corresponding to a current of 10 μA/cm^2) and threshold field (7.38 V/μm, corresponding to current of 1 mA/cm^2), compared to the edges. Fowler-Nordheim (FN) analysis indicates that the basal plane has larger field enhanced factor (1374, while 453 for edges), but smaller emission area efficiency (1.24×10^{-3}) than the edges (0.526). Characterizations show that the sparse wrinkles on the basal plane play important roles as emission sites; the oxygen-containing groups which tend to form on the edges lead to an increase in work function and the deterioration in field emission performance.

1. Introduction

With large aspect ratios, carbon nanotubes (CNTs) have been considered as promising electron-field-emission cathode [1–3], since the demonstration in 1995 [4]. With similar basic structure (sp^2 bonded carbon layers), graphene has also attracted attention for field emission due to the atomic thickness, excellent electrical and thermal conductivities, and good mechanical stability [5–7]. Especially, when the carbon edges were used as electron emission sites, the field emission of protruding graphene layers have been considerably investigated [8–10].

Both surface morphology and electronic structure (e.g., work function) of cathodes are critical for extraordinary field emission (FE) performance [11–13]. Graphene with wrinkles or fins have been demonstrated to exhibit outstanding FE performance, as the wrinkles or fins were considered as high-efficiency emission sites [12,14]. On the other hand, graphene films prepared from exfoliated graphite by spray-coating [11], electrophoretic deposition [8,15] and hydraulic press [16], have been extensively studied for field emission; it was found that the presence of graphene edges was also a key for the excellent FE properties. Numerous studies suggested that lots of exposed edges in vertically-standing graphene could potentially provide a high-density FE sites, and orderly-standing graphene sheets with a proper spatial arrangement

* Corresponding author.
E-mail address: zhuyanwu@ustc.edu.cn (Y. Zhu).

https://doi.org/10.1016/j.matchemphys.2018.01.055
0254-0584/

showed a superior FE performance [17–22]. Other factors influencing the FE performance of graphene-based materials were also investigated. For example, a simulation suggested that the graphene edge saturated with O atoms has the higher work function, compared to that with carbon dangling atoms or that terminated with H [23,24]. Adatom doping such as nitrogen and boron doping, has been shown to have significant effects on the electronic structure and work function of graphene [25–27]; N-doped graphene showed better FE properties than B-doped graphene [28]. Most studies mentioned above, however, have been performed on samples in different morphology or structure, possibly resulting in ambiguous conclusions when the effects of morphology, work function and functional groups are considered simultaneously. Ideally, the FE property of the basal plane shall be compared to that of the edges from the same sample, better with tunable work function. But it is challenging to prepare well-defined basal plane and edges consisting of graphene layers [22,29], and the coexistence of basal plane and edges in randomly oriented graphene samples (e.g., those from graphene powders) has hindered the further understanding of factors determining FE performance [8,14,16]. Previous studies have suggested that the electrons can be emitted from both the basal plane and the edge of graphene [9,29]; while few research have been conducted on the comparative research of FE properties for basal plane and edges from the same graphite sample. Therefore, systematical studies are needed to distinguish the contribution from the basal plane and the edges.

Herein, we report the FE studies of graphite made from graphite oxide (GO), with well-defined basal plane and cross-sectional edges. The graphite made in this way has a flat (002) plane while with randomly distributed wrinkles. The cross-sectional edges consist of lots of protruding graphene or thin-graphite layers. The FE measurement coupled with characterizations show that the sparse wrinkles on the basal plane play the more important role as emission sites than dense protruding edges, although the basal plane has the slightly higher work function than that of clean edges. The oxygen functionalization further increases the work function of the edges and thus deteriorates the FE performance.

2. Experimental

GO was prepared by modified Hummers' method [30]. The graphite samples were made following the method described in our previous report [31]. In brief, the films prepared from graphite oxide slurry were dried, pre-annealed at 1000 °C for 30 min and further calcined at 2950 °C for 2 h in an argon atmosphere. After cooling down to the room temperature, the films were rolled at 150 MPa to obtain the graphite. The as-prepared bulk graphite was cut into slices (as shown in the inset of Fig. 1(a)) with a typical thickness of 2 mm by a diamond wire saws. In order to expose the edges, the cross-section was successively processed by tape-stripping, ultrasonic (30 min) and Ar plasma (100 W, 30 min). The fresh basal plane was obtained by directly splitting the as-prepared graphite with a blade. Prior to characterizations and FE testing, the edges and basal plane samples were annealed at 1000 °C for 2 h in an argon and hydrogen mixture atmosphere. The surface morphology of samples was characterized with scanning electron microscopy (SEM, JSM-6700F) and atomic force microscopy (AFM, Park XE7). The structural characterizations were carried out using X-ray diffraction (XRD, D/max-TTR III) with Cu K_a radiation (V = 40 kV, I = 200 mA) and Raman spectroscopy (Renishaw inVia Raman Microscope, 532 nm laser, 5 mW). X-ray photoelectron spectroscopy (XPS, ESCALAB 250) and ultraviolet photoelectron spectroscopy (UPS, ESCALAB 250, Helium (He) I (21.22eV) irradiation) were utilized to investigate the surface chemical groups and work function of the samples. The FE measurements of the samples were carried out in an ultrahigh vacuum chamber with a pressure lower than 5×10^{-5} pa using a two-parallel-plate configuration by exposing the basal plane or cross-sectional edges to the anode. The distance between cathode and anode was 400 μm or 150 μm for the basal plane or edges sample, respectively. FE current was measured as a function of applied voltage using digital multimeter (Fluke 8808A) and high voltage DC power supply (Teslaman TD2202).

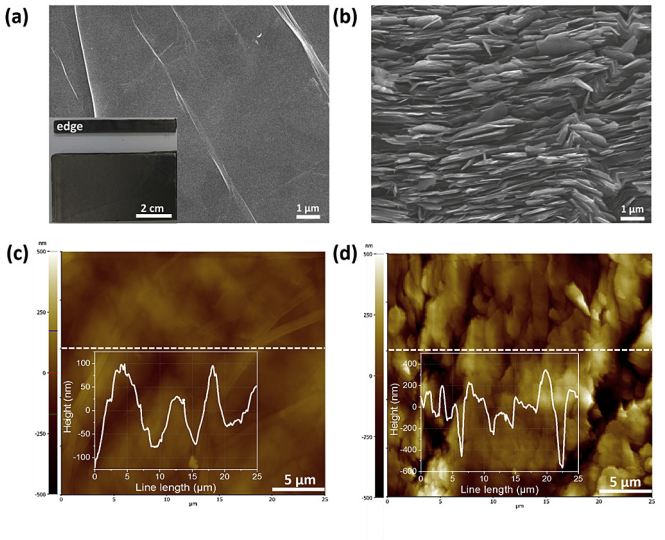

Fig. 1. Typical morphology of the graphite sample. (a) SEM image of the basal plane. Inset shows the photograph of graphite samples, (b) SEM image of cross-sectional edges, (c) AFM image of the basal plane, and (d) AFM image of cross-sectional edges. Insets of (c) and (d) show the corresponding line profiles along the dashed lines.

3. Results and discussion

The method mentioned above allows for the preparation of graphite with size of up to A4 size; typical samples are shown in the inset of Fig. 1(a). Fig. 1(a) is typical SEM image of the basal plane, in which the wrinkles can be clearly identified. The SEM image of cross-sectional edges in Fig. 1(b) shows the orderly layer-by-layer stacking with a small amount of twisting and bending of layers. From the corresponding AFM image of the basal plane (Fig. 1(c)), a roughness (root mean square, Rms) of 0.04 μm is obtained. The line profile shown in the inset indicates that the height of wrinkles ranges from 0.10 to 0.17 μm. As the wrinkles are randomly distributed on the basal plane, the distance between wrinkles shown in the AFM image are roughly estimated as several micrometers. From the profile we can also see that the width of the wrinkles spreads to a scale of micrometers, partially caused by the limitation of lateral resolution of AFM tips. From the AFM image and the line profile shown in Fig. 1(d), larger Rms roughness of 0.23 μm is obtained from the cross-sectional edges. The protruding height of the edges ranges between 0.03 μm and 0.55 μm. The distance between adjacent protrusions is much smaller than that between wrinkles shown in Fig. 1(a), while the individual graphene layers can not be distinguished because of close stacking of the layers. The density of as-prepared graphite sample is 2.19 g/cm^3, slightly smaller than 2.26 g/cm^3 of graphite.

Raman spectra shown in Fig. 2(a) further display the difference between the basal plane and the cross-sectional edges. The D peak (1350 cm^{-1}) and the shoulder (1620 cm^{-1}) next to G peak associated with topological and disorder defects, can been clearly seen from spectrum of the edges [32], while hardly found from that of the basal plane. The result indicates that the edges consist of a large

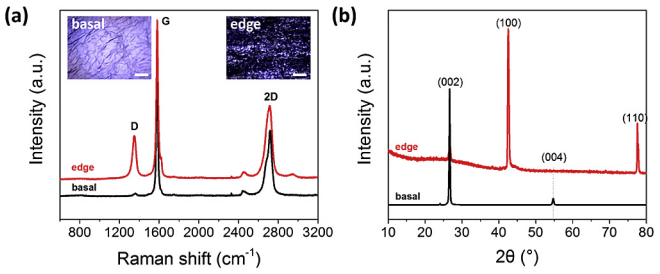

Fig. 2. (a) Raman spectra of the basal plane and cross-sectional edges. Insets show the optical micro photographs for each sample. Scale bars: 20 μm. (b) XRD patterns obtained from the basal plane and cross-sectional edges.

number of topological defects. The G (1580 cm^{-1}) and 2D (2715 cm^{-1}) peaks obtained from both the basal plane and the edges are similar to those in graphite [32,33]. The asymmetric 2D peak, especially from the basal plane, is a clear indication of Bernal stacking [34]. The XRD patterns of the basal plane and edges are shown in Fig. 2(b). The diffraction peaks of both samples are close to those of 2H-graphite (JCPDS#41-1487). Two peaks corresponding to (002) and (004) interlayer distances can be identified from the basal plane, while (002), (100) and (110) planes are observed from the edges. The fact that the strong diffractions of (100) and (110) planes are only observed from the edges indicates the high-order orientation of the graphite made from graphite oxide.

Fig. 3(a) shows the FE current density versus electric field (J-E) curves measured from the basal plane and the edges. To investigate the oxygen-doping effects on the graphene edges caused by exposure of samples in anbience [35], another sample with edges exposed in air for a month (named O-edges) was also measured for comparison. From the J-E curves, the turn-on electric field (E_{to}) (defined as the electric field corresponding to a FE current of 10 μA/cm^2) is 5.01, 10.59, and 17.34 V/μm, for the basal plane, edges and O-edges, respectively. Accordingly, the threshold field (E_{th}) (the field corresponding to 1 mA/cm^2) is 7.38, 13.12, and 25.16 V/μm for the basal plane, edges, and O-edges. The E_{to} for basal plane is lower than that of well-aligned graphene arrays [29] and few-layer graphene film [11], but higher than the values reported for graphene fins [14] and disordered monolayer graphene [12]. The Fowler-Nordheim (FN) equation [36] is employed to further analyze the FE behavior [37],

$$\ln\left(\frac{J}{E^2}\right) = \ln\left(\frac{A\alpha\beta^2}{\varnothing}\right) + \frac{BC^2}{\sqrt{\varnothing}} - \frac{B\varnothing^{\frac{3}{2}}}{\beta E} \quad (1)$$

where Φ is the work function, A, B, and C^2 are constants with values $A = 1.54 \times 10^{-6}$ A eV V^{-2}, $B = 6.83 \times 10^{7}$ V $eV^{-3/2}$ cm^{-1}, and $C^2 = 4.43 \times 10^{-7}$ eV^2 cm V^{-1}. The factor β (field enhanced factor) indicates the amplifying aptitude of the emitter to the electric field, and the parameter α is called the emission area efficiency, which is defined as the ratio of the effective emission area to the geometrical area of the emitter. Fig. 3(b) shows the FN curves ($Ln(J/E^2)$ versus 1/E), from which β and α can be obtained by fitting the curves when Φ is known. As we can see that, the FN plots for all three samples can be fitted as two linear sections with distinct slopes in low-field (I) and high-field (II) regions. A field emission tunneling dominates in region I and hot electrons may be excited at high electric field (region II) [13,14]. Thus the values of β and α are calculated from the FN plots in Region I are shown in Table 1 by using the work function values measured from UPS. As can be seen, the basal plane has the largest β (1374) while the smallest emission area efficiency α (1.24×10^{-3}) among all samples, which manifests the relatively smaller effective emission area of the basal plane. Based on the estimation of the area of wrinkles from AFM image (the ratio of wrinkle area to the geometrical area for the basal plane is ~1.00×10^{-2}), it can be inferred that the emission is mainly from the wrinkles [12,14]. On the other hand, the bigger α value of edges suggests that more than half of the edges are involved in electron emission while with small emission current in average.

To investigate the roles of surface chemistry in addition to geometrical morphology [13,23,24], XPS and UPS were carried out on the samples and the spectra are shown in Fig. 4. From the XPS spectra shown in Fig. 4(a), a prominent O 1s (533 eV) peak is observed from the edges and O-edges, due to the existence of oxygen-containing groups. The oxygen content for the basal plane, edges and O-edges is estimated as 0.34 at. %, 4.71 at. % and 11.37 at. %, respectively. The C 1s spectra in Fig. 4(b) show the main peak at 284.5 eV and a weak peak at 285.6 eV, corresponding to the sp^2 and sp^3 carbon bonding respectively [38]. Those peaks with higher binding energies, e.g., located at 287.0 eV and 288.6 eV are considered from C-O and O-C=O bonds [38,39]. These results show the plenty of oxygen groups formed on the O-edges. The work function (Φ) is estimated by analyzing the width between the analyzer Fermi level (E_{fermi}) and the high binding energy cutoff (E_{cutoff}) from the UPS spectra in Fig. 4(c) [13,38]. Fig. 4(d) shows a detailed spectra of cutoff region, and the method of E_{cutoff} estimation has been described in previous report [40]. Among the three

Table 1
FE properties and work function of the graphite samples.

Samples	E_{to} (V/μm)	E_{th} (V/μm)	β (I)	α (I)	E_{fermi} (eV)	E_{cutoff} (eV)	Φ (eV)
Basal	5.01	7.38	1374	1.24×10^{-3}	2.92	18.33	5.81
Edges	10.59	13.12	453	0.526	2.88	18.49	5.61
O-edges	17.34	25.16	304	0.094	2.89	17.81	6.30

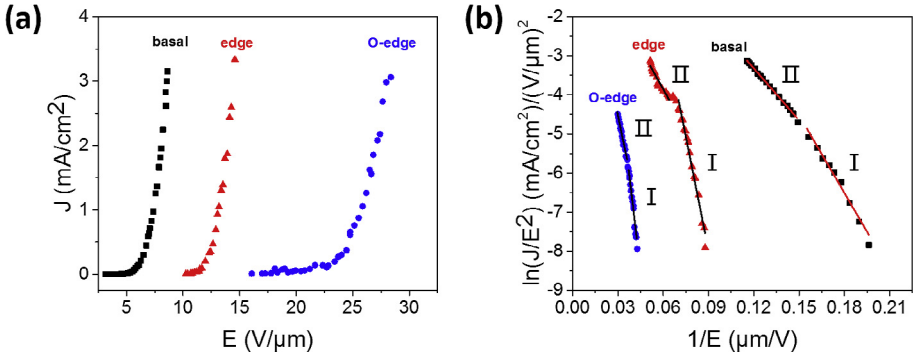

Fig. 3. (a) Field emission J-E curves, (b) Corresponding FN plots of the basal plane, cross-sectional edges and O-edges.

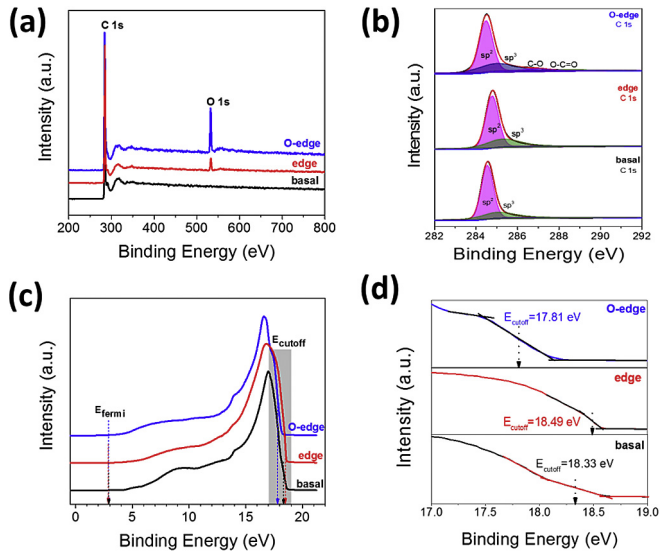

Fig. 4. (a) XPS survey spectra, (b) C 1s XPS spectra, (c) UPS spectra, and (d) Detailed spectra in the cutoff region for the basal plane, cross-sectional edges and O-edges.

samples, the fresh edges have the largest E_{cutoff} (18.49 eV), leading to a work function (5.61 eV) smaller than that of the basal plane (5.81 eV), which might be attributed to the armchair edge or H-terminated carbon atoms in the edges [24,41]. Comparatively the O-edges have much larger Φ (6.30 eV) due to the oxygen groups, consistent to previous reports [23,24], which may explain the inferior FE performance of O-edges among the three samples.

4. Conclusion

In summary, the morphological and chemical factors influencing FE properties of graphite made from GO have been investigated by comparing the performances of basal plane and cross-sectional edges. Likely because of high-density adjacent edge sites which interfere with each other, the edges have demonstrated inferior FE performance even with the smaller work function. The oxygen groups on the edges have further deteriorated the performance. In contrast, the basal plane with sparse wrinkles has demonstrated superior FE property, indicated by lower turn-on field and threshold field, despite of the smaller area efficiency. The result may shed light on the design of graphene- or graphite-based FE cathodes for further improved performance in future.

Acknowledgments

We acknowledge financial support from the China Government 1000 Plan Talent Program, the China MOE NCET Program, the Natural Science Foundation of China (51322204, 51772282), the Fundamental Research Funds for the Central Universities (WK2060140014 and WK2060140017), and the Technological Development Grant of Hefei Science Center of CAS (2014TDG-HSC002).

References

[1] J.-M. Bonard, K.A. Dean, B.F. Coll, C. Klinke, Field emission of individual carbon nanotubes in the scanning electron microscope, Phys. Rev. Lett. 89 (2002), 197602.
[2] E. Minoux, O. Groening, K.B. Teo, S.H. Dalal, L. Gangloff, J.-P. Schnell, L. Hudanski, I.Y. Bu, P. Vincent, P. Legagneux, Achieving high-current carbon nanotube emitters, Nano Lett. 5 (2005) 2135–2138.
[3] S.M. Jung, J. Hahn, H.Y. Jung, J.S. Suh, Clean carbon nanotube field emitters aligned horizontally, Nano Lett. 6 (2006) 1569–1573.
[4] W.A. De Heer, A. Chatelain, D. Ugarte, A carbon nanotube field-emission electron source, Science 270 (1995) 1179–1181.
[5] K.S. Novoselov, A.K. Geim, S.V. Morozov, D. Jiang, Y. Zhang, S.V. Dubonos, I.V. Grigorieva, A.A. Firsov, Electric field effect in atomically thin carbon films, Science 306 (2004) 666–669.
[6] A.K. Geim, K.S. Novoselov, The rise of graphene, Nat. Mater. 6 (2007) 183–191.
[7] Y. Kopelevich, P. Esquinazi, Graphene physics in graphite, Adv. Mater. 19 (2007) 4559–4563.
[8] Z.-S. Wu, S. Pei, W. Ren, D. Tang, L. Gao, B. Liu, F. Li, C. Liu, H.-M. Cheng, Field emission of single-layer graphene films prepared by electrophoretic deposition, Adv. Mater. 21 (2009) 1756–1760.
[9] X. Wei, Y. Bando, D. Golberg, Electron emission from individual graphene nanoribbons driven by internal electric field, ACS Nano 6 (2011) 705–711.
[10] J. Liu, B. Zeng, W. Wang, N. Li, J. Guo, Graphene electron cannon: high-current edge emission from aligned graphene sheets, Appl. Phys. Lett. 104 (2014), 023101.
[11] J. Li, J. Chen, B. Shen, X. Yan, Q. Xue, Temperature dependence of the field emission from the few-layer graphene film, Appl. Phys. Lett. 99 (2011), 163103.
[12] S. Pandey, P. Rai, S. Patole, F. Gunes, G.-D. Kwon, J.-B. Yoo, P. Nikolaev, S. Arepalli, Improved electron field emission from morphologically disordered monolayer graphene, Appl. Phys. Lett. 100 (2012), 043104.
[13] T. Yamada, T. Masuzawa, T. Ebisudani, K. Okano, T. Taniguchi, Field emission characteristics from graphene on hexagonal boron nitride, Appl. Phys. Lett. 104 (2014), 221603.
[14] T. Hallam, M.T. Cole, W.I. Milne, G.S. Duesberg, Field emission characteristics of contact printed graphene fins, Small 10 (2014) 95–99.
[15] J. Chen, J. Li, J. Yang, X. Yan, B.-K. Tay, Q. Xue, The hysteresis phenomenon of the field emission from the graphene film, Appl. Phys. Lett. 99 (2011), 173104.
[16] R.T. Khare, R.V. Gelamo, M.A. More, D.J. Late, C.S. Rout, Enhanced field emission of plasma treated multilayer graphene, Appl. Phys. Lett. 107 (2015), 123503.
[17] L. Jiang, T. Yang, F. Liu, J. Dong, Z. Yao, C. Shen, S. Deng, N. Xu, Y. Liu, H.J. Gao, Controlled synthesis of large-scale, uniform, vertically standing graphene for high-performance field emitters, Adv. Mater. 25 (2013) 250–255.
[18] S.K. Behura, I. Mukhopadhyay, A. Hirose, Q. Yang, O. Jani, Vertically oriented few-layer graphene as an electron field-emitter, Phys. Status Solidi A 210 (2013) 1817–1821.
[19] A. Malesevic, R. Kemps, A. Vanhulsel, M.P. Chowdhury, A. Volodin, C. Van Haesendonck, Field emission from vertically aligned few-layer graphene, J. Appl. Phys. 104 (2008), 084301.
[20] C. Wu, F. Li, Y. Zhang, T. Guo, Field emission from vertical graphene sheets formed by screen-printing technique, Vacuum 94 (2013) 48–52.
[21] Y. Zhang, J. Du, S. Tang, P. Liu, S. Deng, J. Chen, N. Xu, Optimize the field emission character of a vertical few-layer graphene sheet by manipulating the morphology, Nanotechnology 23 (2012), 015202.
[22] J.T. Tsai, T.Y. Chu, J.Y. Shiu, C.S. Yang, Field emission from an individual free-standing graphene edge, Small 8 (2012) 3739–3745.
[23] W. Wang, Z. Li, Potential barrier of graphene edges, J. Appl. Phys. 109 (2011), 114308.
[24] R. Ramprasad, P.v. Allmen, L.R.C. Fonseca, Contributions to the work function: a density-functional study of adsorbates at graphene ribbon edges, Phys. Rev. B 60 (1999) 6023.
[25] K. Akada, T.-o. Terasawa, G. Imamura, S. Obata, K. Saiki, Control of work function of graphene by plasma assisted nitrogen doping, Appl. Phys. Lett. 104 (2014), 131602.
[26] W.-C. Yen, H. Medina, J.-S. Huang, C.-C. Lai, Y.-C. Shih, S.-M. Lin, J.-G. Li, Z.M. Wang, Y.-L. Chueh, Direct synthesis of graphene with tunable work function on insulators via in situ boron doping by nickel-assisted growth, J. Phys. Chem. C 118 (2014) 25089–25096.
[27] L. Miao, R. Jia, Y. Wang, C.-P. Kong, J. Wang, R.I. Eglitis, H.-X. Zhang, Certain doping concentrations caused half-metallic graphene, J. Saudi Chem. Soc. 21 (2017) 111–117.
[28] U.A. Palnitkar, R.V. Kashid, M.A. More, D.S. Joag, L.S. Panchakarla, C.N.R. Rao, Remarkably low turn-on field emission in undoped, nitrogen-doped, and boron-doped graphene, Appl. Phys. Lett. 97 (2010), 063102.
[29] C.-K. Huang, Y. Ou, Y. Bie, Q. Zhao, D. Yu, Well-aligned graphene arrays for field emission displays, Appl. Phys. Lett. 98 (2011), 263104.
[30] W.S. Hummers Jr., R.E. Offeman, Preparation of graphitic oxide, J. Am. Chem. Soc. 80 (1958), 1339–1339.
[31] Z. Tan, H. Xu, B. Zhou, Z. Qi, Y. Qu, Y. Zhu, Planar lighting from optimized graphite papers made of graphite oxide, Appl. Phys. Lett. 110 (2017), 211903.
[32] M.S. Dresselhaus, A. Jorio, M. Hofmann, G. Dresselhaus, R. Saito, Perspectives on carbon nanotubes and graphene Raman spectroscopy, Nano Lett. 10 (2010) 751–758.
[33] A.C. Ferrari, J.C. Meyer, V. Scardaci, C. Casiraghi, M. Lazzeri, F. Mauri, S. Piscanec, D. Jiang, K.S. Novoselov, S. Roth, A.K. Geim, Raman spectrum of graphene and graphene layers, Phys. Rev. Lett. 97 (2006), 187401.
[34] B. Jouault, B. Jabakhanji, N. Camara, W. Desrat, A. Tiberj, J.-R. Huntzinger, C. Consejo, A. Caboni, P. Godignon, Y. Kopelevich, Probing the electrical anisotropy of multilayer graphene on the Si face of 6 H-SiC, Phys. Rev. B 82 (2010) 085438.
[35] Y. Yang, R. Murali, Binding mechanisms of molecular oxygen and moisture to graphene, Appl. Phys. Lett. 98 (2011), 093116.
[36] R.H. Fowler, L. Nordheim, Electron emission in intense electric fields, in:

Proceedings of the Royal Society of London A: Mathematical, Physical and Engineering Sciences, The Royal Society, 1928, pp. 173–181.
[37] A. Obraztsov, A.A. Zakhidov, A. Volkov, D. Lyashenko, Non-classical electron field emission from carbon materials, Diam. Relat. Mater. 12 (2003) 446–449.
[38] A. Siokou, F. Ravani, S. Karakalos, O. Frank, M. Kalbac, C. Galiotis, Surface refinement and electronic properties of graphene layers grown on copper substrate: an XPS, UPS and EELS study, Appl. Surf. Sci. 257 (2011) 9785–9790.
[39] H. Ago, T. Kugler, F. Cacialli, W.R. Salaneck, M.S. Shaffer, A.H. Windle, R.H. Friend, Work functions and surface functional groups of multiwall carbon nanotubes, J. Phys. Chem. B 103 (1999) 8116–8121.
[40] Y. Park, V. Choong, Y. Gao, B.R. Hsieh, C.W. Tang, Work function of indium tin oxide transparent conductor measured by photoelectron spectroscopy, Appl. Phys. Lett. 68 (1996) 2699–2701.
[41] W. Wang, X. Qin, N. Xu, Z. Li, Field electron emission characteristic of graphene, J. Appl. Phys. 109 (2011) 044304–044307.